



Search for Leptoquark Pairs Decaying to $\nu\nu + \text{jets}$ in $p\bar{p}$ Collisions at $\sqrt{s}=1.8$ TeV

V.M. Abazov,²³ B. Abbott,⁵⁷ A. Abdesselam,¹¹ M. Abolins,⁵⁰ V. Abramov,²⁶
B.S. Acharya,¹⁷ D.L. Adams,⁵⁹ M. Adams,³⁷ S.N. Ahmed,²¹ G.D. Alexeev,²³ A. Alton,⁴⁹
G.A. Alves,² N. Amos,⁴⁹ E.W. Anderson,⁴² Y. Arnoud,⁹ C. Avila,⁵ M.M. Baarmand,⁵⁴
V.V. Babintsev,²⁶ L. Babukhadia,⁵⁴ T.C. Bacon,²⁸ A. Baden,⁴⁶ B. Baldin,³⁶ P.W. Balm,²⁰
S. Banerjee,¹⁷ E. Barberis,³⁰ P. Baringer,⁴³ J. Barreto,² J.F. Bartlett,³⁶ U. Bassler,¹²
D. Bauer,²⁸ A. Bean,⁴³ F. Beaudette,¹¹ M. Begel,⁵³ A. Belyaev,³⁵ S.B. Beri,¹⁵
G. Bernardi,¹² I. Bertram,²⁷ A. Besson,⁹ R. Beuselinck,²⁸ V.A. Bezubov,²⁶ P.C. Bhat,³⁶
V. Bhatnagar,¹⁵ M. Bhattacharjee,⁵⁴ G. Blazey,³⁸ F. Blekman,²⁰ S. Blessing,³⁵
A. Boehnlein,³⁶ N.I. Bojko,²⁶ F. Borcherding,³⁶ K. Bos,²⁰ T. Bose,⁵² A. Brandt,⁵⁹
R. Breedon,³¹ G. Briskin,⁵⁸ R. Brock,⁵⁰ G. Brooijmans,³⁶ A. Bross,³⁶ D. Buchholz,³⁹
M. Buehler,³⁷ V. Buescher,¹⁴ V.S. Burtovoi,²⁶ J.M. Butler,⁴⁷ F. Canelli,⁵³ W. Carvalho,³
D. Casey,⁵⁰ Z. Casilum,⁵⁴ H. Castilla-Valdez,¹⁹ D. Chakraborty,³⁸ K.M. Chan,⁵³
S.V. Chekulaev,²⁶ D.K. Cho,⁵³ S. Choi,³⁴ S. Chopra,⁵⁵ J.H. Christenson,³⁶ M. Chung,³⁷
D. Claes,⁵¹ A.R. Clark,³⁰ L. Coney,⁴¹ B. Connolly,³⁵ W.E. Cooper,³⁶ D. Coppage,⁴³
S. Crépé-Renaudin,⁹ M.A.C. Cummings,³⁸ D. Cutts,⁵⁸ G.A. Davis,⁵³ K. Davis,²⁹ K. De,⁵⁹
S.J. de Jong,²¹ K. Del Signore,⁴⁹ M. Demarteau,³⁶ R. Demina,⁴⁴ P. Demine,⁹ D. Denisov,³⁶
S.P. Denisov,²⁶ S. Desai,⁵⁴ H.T. Diehl,³⁶ M. Diesburg,³⁶ S. Doulas,⁴⁸ Y. Ducros,¹³
L.V. Dudko,²⁵ S. Duensing,²¹ L. Duflot,¹¹ S.R. Dugad,¹⁷ A. Duperrin,¹⁰ A. Dyshkant,³⁸
D. Edmunds,⁵⁰ J. Ellison,³⁴ J.T. Eltzroth,⁵⁹ V.D. Elvira,³⁶ R. Engelmann,⁵⁴ S. Eno,⁴⁶
G. Eppley,⁶¹ P. Ermolov,²⁵ O.V. Eroshin,²⁶ J. Estrada,⁵³ H. Evans,⁵² V.N. Evdokimov,²⁶
T. Fahland,³³ S. Feher,³⁶ D. Fein,²⁹ T. Ferbel,⁵³ F. Filthaut,²¹ H.E. Fisk,³⁶ Y. Fisyak,⁵⁵
E. Flattum,³⁶ F. Fleuret,¹² M. Fortner,³⁸ H. Fox,³⁹ K.C. Frame,⁵⁰ S. Fu,⁵² S. Fuess,³⁶
E. Gallas,³⁶ A.N. Galyaev,²⁶ M. Gao,⁵² V. Gavrilov,²⁴ R.J. Genik II,²⁷ K. Genser,³⁶
C.E. Gerber,³⁷ Y. Gershtein,⁵⁸ R. Gilmartin,³⁵ G. Ginther,⁵³ B. Gómez,⁵ G. Gómez,⁴⁶
P.I. Goncharov,²⁶ J.L. González Solís,¹⁹ H. Gordon,⁵⁵ L.T. Goss,⁶⁰ K. Gounder,³⁶
A. Goussiou,²⁸ N. Graf,⁵⁵ G. Graham,⁴⁶ P.D. Grannis,⁵⁴ J.A. Green,⁴² H. Greenlee,³⁶
Z.D. Greenwood,⁴⁵ S. Grinstein,¹ L. Groer,⁵² S. Grünendahl,³⁶ A. Gupta,¹⁷
S.N. Gurzhiev,²⁶ G. Gutierrez,³⁶ P. Gutierrez,⁵⁷ N.J. Hadley,⁴⁶ H. Haggerty,³⁶
S. Hagopian,³⁵ V. Hagopian,³⁵ R.E. Hall,³² P. Hanlet,⁴⁸ S. Hansen,³⁶ J.M. Hauptman,⁴²
C. Hays,⁵² C. Hebert,⁴³ D. Hedin,³⁸ J.M. Heinmiller,³⁷ A.P. Heinson,³⁴ U. Heintz,⁴⁷
M.D. Hildreth,⁴¹ R. Hirosky,⁶² J.D. Hobbs,⁵⁴ B. Hoeneisen,⁸ Y. Huang,⁴⁹ I. Iashvili,³⁴
R. Illingworth,²⁸ A.S. Ito,³⁶ M. Jaffré,¹¹ S. Jain,¹⁷ R. Jesik,²⁸ K. Johns,²⁹ M. Johnson,³⁶
A. Jonckheere,³⁶ H. Jöstlein,³⁶ A. Juste,³⁶ W. Kahl,⁴⁴ S. Kahn,⁵⁵ E. Kajfasz,¹⁰
A.M. Kalinin,²³ D. Karmanov,²⁵ D. Karmgard,⁴¹ R. Kehoe,⁵⁰ A. Khanov,⁴⁴
A. Kharchilava,⁴¹ S.K. Kim,¹⁸ B. Klíma,³⁶ B. Knuteson,³⁰ W. Ko,³¹ J.M. Kohli,¹⁵
A.V. Kostritskiy,²⁶ J. Kotcher,⁵⁵ B. Kothari,⁵² A.V. Kotwal,⁵² A.V. Kozelov,²⁶
E.A. Kozlovsky,²⁶ J. Krane,⁴² M.R. Krishnaswamy,¹⁷ P. Krivkova,⁶ S. Krzywdzinski,³⁶
M. Kubantsev,⁴⁴ S. Kuleshov,²⁴ Y. Kulik,⁵⁴ S. Kunori,⁴⁶ A. Kupco,⁷ V.E. Kuznetsov,³⁴
G. Landsberg,⁵⁸ W.M. Lee,³⁵ A. Leflat,²⁵ C. Leggett,³⁰ F. Lehner,^{36,*} C. Leonidopoulos,⁵²
J. Li,⁵⁹ Q.Z. Li,³⁶ X. Li,⁴ J.G.R. Lima,³ D. Lincoln,³⁶ S.L. Linn,³⁵ J. Linnemann,⁵⁰

R. Lipton,³⁶ A. Lucotte,⁹ L. Lueking,³⁶ C. Lundstedt,⁵¹ C. Luo,⁴⁰ A.K.A. Maciel,³⁸
 R.J. Madaras,³⁰ V.L. Malyshev,²³ V. Manankov,²⁵ H.S. Mao,⁴ T. Marshall,⁴⁰
 M.I. Martin,³⁸ K.M. Mauritz,⁴² A.A. Mayorov,⁴⁰ R. McCarthy,⁵⁴ T. McMahon,⁵⁶
 H.L. Melanson,³⁶ M. Merkin,²⁵ K.W. Merritt,³⁶ C. Miao,⁵⁸ H. Miettinen,⁶¹ D. Mihalcea,³⁸
 C.S. Mishra,³⁶ N. Mokhov,³⁶ N.K. Mondal,¹⁷ H.E. Montgomery,³⁶ R.W. Moore,⁵⁰
 M. Mostafa,¹ H. da Motta,² E. Nagy,¹⁰ F. Nang,²⁹ M. Narain,⁴⁷ V.S. Narasimham,¹⁷
 N.A. Naumann,²¹ H.A. Neal,⁴⁹ J.P. Negret,⁵ S. Negroni,¹⁰ T. Nunnemann,³⁶ D. O'Neil,⁵⁰
 V. Oguri,³ B. Olivier,¹² N. Oshima,³⁶ P. Padley,⁶¹ L.J. Pan,³⁹ K. Papageorgiou,³⁷
 A. Para,³⁶ N. Parashar,⁴⁸ R. Partridge,⁵⁸ N. Parua,⁵⁴ M. Paterno,⁵³ A. Patwa,⁵⁴
 B. Pawlik,²² J. Perkins,⁵⁹ O. Peters,²⁰ P. Pétroff,¹¹ R. Piegaia,¹ B.G. Pope,⁵⁰ E. Popkov,⁴⁷
 H.B. Prosper,³⁵ S. Protopopescu,⁵⁵ M.B. Przybycien,^{39,†} J. Qian,⁴⁹ R. Raja,³⁶
 S. Rajagopalan,⁵⁵ E. Ramberg,³⁶ P.A. Rapidis,³⁶ N.W. Reay,⁴⁴ S. Reucroft,⁴⁸ M. Ridel,¹¹
 M. Rijssenbeek,⁵⁴ F. Rizatdinova,⁴⁴ T. Rockwell,⁵⁰ M. Roco,³⁶ C. Royon,¹³ P. Rubinov,³⁶
 R. Ruchti,⁴¹ J. Rutherford,²⁹ B.M. Sabirov,²³ G. Sajot,⁹ A. Santoro,² L. Sawyer,⁴⁵
 R.D. Schamberger,⁵⁴ H. Schellman,³⁹ A. Schwartzman,¹ N. Sen,⁶¹ E. Shabalina,³⁷
 R.K. Shivpuri,¹⁶ D. Shpakov,⁴⁸ M. Shupe,²⁹ R.A. Sidwell,⁴⁴ V. Simak,⁷ H. Singh,³⁴
 J.B. Singh,¹⁵ V. Sirotenko,³⁶ P. Slattery,⁵³ E. Smith,⁵⁷ R.P. Smith,³⁶ R. Snihur,³⁹
 G.R. Snow,⁵¹ J. Snow,⁵⁶ S. Snyder,⁵⁵ J. Solomon,³⁷ Y. Song,⁵⁹ V. Sorín,¹ M. Sosebee,⁵⁹
 N. Sotnikova,²⁵ K. Soustruznik,⁶ M. Souza,² N.R. Stanton,⁴⁴ G. Steinbrück,⁵²
 R.W. Stephens,⁵⁹ F. Stichelbaut,⁵⁵ D. Stoker,³³ V. Stolin,²⁴ A. Stone,⁴⁵ D.A. Stoyanova,²⁶
 M.A. Strang,⁵⁹ M. Strauss,⁵⁷ M. Strovink,³⁰ L. Stutte,³⁶ A. Sznajder,³ M. Talby,¹⁰
 W. Taylor,⁵⁴ S. Tentindo-Repond,³⁵ S.M. Tripathi,³¹ T.G. Trippe,³⁰ A.S. Turcot,⁵⁵
 P.M. Tuts,⁵² V. Vaniev,²⁶ R. Van Kooten,⁴⁰ N. Varelas,³⁷ L.S. Vertogradov,²³
 F. Villeneuve-Seguier,¹⁰ A.A. Volkov,²⁶ A.P. Vorobiev,²⁶ H.D. Wahl,³⁵ H. Wang,³⁹
 Z.-M. Wang,⁵⁴ J. Warchol,⁴¹ G. Watts,⁶³ M. Wayne,⁴¹ H. Weerts,⁵⁰ A. White,⁵⁹
 J.T. White,⁶⁰ D. Whiteson,³⁰ D.A. Wijngaarden,²¹ S. Willis,³⁸ S.J. Wimpenny,³⁴
 J. Womersley,³⁶ D.R. Wood,⁴⁸ Q. Xu,⁴⁹ R. Yamada,³⁶ P. Yamin,⁵⁵ T. Yasuda,³⁶
 Y.A. Yatsunenko,²³ K. Yip,⁵⁵ S. Youssef,³⁵ J. Yu,³⁶ Z. Yu,³⁹ M. Zanabria,⁵ X. Zhang,⁵⁷
 H. Zheng,⁴¹ B. Zhou,⁴⁹ Z. Zhou,⁴² M. Zielinski,⁵³ D. Zieminska,⁴⁰ A. Zieminski,⁴⁰
 V. Zutshi,⁵⁵ E.G. Zverev,²⁵ and A. Zylberstejn¹³

(DØ Collaboration)

¹*Universidad de Buenos Aires, Buenos Aires, Argentina*

²*LAFEX, Centro Brasileiro de Pesquisas Físicas, Rio de Janeiro, Brazil*

³*Universidade do Estado do Rio de Janeiro, Rio de Janeiro, Brazil*

⁴*Institute of High Energy Physics, Beijing, People's Republic of China*

⁵*Universidad de los Andes, Bogotá, Colombia*

⁶*Charles University, Center for Particle Physics, Prague, Czech Republic*

⁷*Institute of Physics, Academy of Sciences, Center for Particle Physics, Prague, Czech Republic*

⁸*Universidad San Francisco de Quito, Quito, Ecuador*

⁹*Institut des Sciences Nucléaires, IN2P3-CNRS, Université de Grenoble 1, Grenoble, France*

¹⁰*CPPM, IN2P3-CNRS, Université de la Méditerranée, Marseille, France*

¹¹*Laboratoire de l'Accélérateur Linéaire, IN2P3-CNRS, Orsay, France*

¹²*LPNHE, Universités Paris VI and VII, IN2P3-CNRS, Paris, France*

- ¹³*DAPNIA/Service de Physique des Particules, CEA, Saclay, France*
- ¹⁴*Universität Mainz, Institut für Physik, Mainz, Germany*
- ¹⁵*Panjab University, Chandigarh, India*
- ¹⁶*Delhi University, Delhi, India*
- ¹⁷*Tata Institute of Fundamental Research, Mumbai, India*
- ¹⁸*Seoul National University, Seoul, Korea*
- ¹⁹*CINVESTAV, Mexico City, Mexico*
- ²⁰*FOM-Institute NIKHEF and University of Amsterdam/NIKHEF, Amsterdam, The Netherlands*
- ²¹*University of Nijmegen/NIKHEF, Nijmegen, The Netherlands*
- ²²*Institute of Nuclear Physics, Kraków, Poland*
- ²³*Joint Institute for Nuclear Research, Dubna, Russia*
- ²⁴*Institute for Theoretical and Experimental Physics, Moscow, Russia*
- ²⁵*Moscow State University, Moscow, Russia*
- ²⁶*Institute for High Energy Physics, Protvino, Russia*
- ²⁷*Lancaster University, Lancaster, United Kingdom*
- ²⁸*Imperial College, London, United Kingdom*
- ²⁹*University of Arizona, Tucson, Arizona 85721*
- ³⁰*Lawrence Berkeley National Laboratory and University of California, Berkeley, California 94720*
- ³¹*University of California, Davis, California 95616*
- ³²*California State University, Fresno, California 93740*
- ³³*University of California, Irvine, California 92697*
- ³⁴*University of California, Riverside, California 92521*
- ³⁵*Florida State University, Tallahassee, Florida 32306*
- ³⁶*Fermi National Accelerator Laboratory, Batavia, Illinois 60510*
- ³⁷*University of Illinois at Chicago, Chicago, Illinois 60607*
- ³⁸*Northern Illinois University, DeKalb, Illinois 60115*
- ³⁹*Northwestern University, Evanston, Illinois 60208*
- ⁴⁰*Indiana University, Bloomington, Indiana 47405*
- ⁴¹*University of Notre Dame, Notre Dame, Indiana 46556*
- ⁴²*Iowa State University, Ames, Iowa 50011*
- ⁴³*University of Kansas, Lawrence, Kansas 66045*
- ⁴⁴*Kansas State University, Manhattan, Kansas 66506*
- ⁴⁵*Louisiana Tech University, Ruston, Louisiana 71272*
- ⁴⁶*University of Maryland, College Park, Maryland 20742*
- ⁴⁷*Boston University, Boston, Massachusetts 02215*
- ⁴⁸*Northeastern University, Boston, Massachusetts 02115*
- ⁴⁹*University of Michigan, Ann Arbor, Michigan 48109*
- ⁵⁰*Michigan State University, East Lansing, Michigan 48824*
- ⁵¹*University of Nebraska, Lincoln, Nebraska 68588*
- ⁵²*Columbia University, New York, New York 10027*
- ⁵³*University of Rochester, Rochester, New York 14627*
- ⁵⁴*State University of New York, Stony Brook, New York 11794*
- ⁵⁵*Brookhaven National Laboratory, Upton, New York 11973*
- ⁵⁶*Langston University, Langston, Oklahoma 73050*
- ⁵⁷*University of Oklahoma, Norman, Oklahoma 73019*

⁵⁸*Brown University, Providence, Rhode Island 02912*

⁵⁹*University of Texas, Arlington, Texas 76019*

⁶⁰*Texas A&M University, College Station, Texas 77843*

⁶¹*Rice University, Houston, Texas 77005*

⁶²*University of Virginia, Charlottesville, Virginia 22901*

⁶³*University of Washington, Seattle, Washington 98195*

Abstract

We present the results of a search for leptoquark (LQ) pairs in (85.2 ± 3.7) pb $^{-1}$ of $p\bar{p}$ collider data collected by the D \emptyset experiment at the Fermilab Tevatron. We observe no evidence for leptoquark production and set a limit on $\sigma(p\bar{p} \rightarrow LQ\overline{LQ} \rightarrow \nu\nu + \text{jets})$ as a function of the mass of the leptoquark (m_{LQ}). Assuming the decay $LQ \rightarrow \nu q$, we exclude scalar leptoquarks for $m_{LQ} < 98$ GeV/ c^2 , and vector leptoquarks for $m_{LQ} < 200$ GeV/ c^2 and coupling which produces the minimum cross section, at a 95% confidence level.

The observed symmetry between the lepton (l) and quark (q) sectors suggests the existence of a force connecting the two that is mediated by leptoquark (LQ) particles that couple directly to both leptons and quarks. Such particles arise naturally as vector [1] or scalar bosons [2] in Grand Unified Theories [1], as composite particles [3], as techniparticles [4], or as R-parity violating supersymmetric particles [5].

Leptoquarks would carry both color and fractional electric charge. They could be pair-produced at the Fermilab Tevatron through a virtual gluon (g) in the strong process $p\bar{p} \rightarrow g \rightarrow LQL\bar{Q} + X$, with a production cross section that, for scalar leptoquarks, is independent of the $LQ - q - l$ coupling. For vector leptoquarks, we consider the specific cases of the coupling resulting in the minimal cross section (σ_{\min}), Minimal Vector coupling (MV), and Yang-Mills coupling (YM) [6].

Limits from flavor-changing neutral currents imply that leptoquarks of low mass $\mathcal{O}(\text{TeV})$ couple only within a single generation [7], and the decays of leptoquark pairs would therefore be expected to yield one of three possible final states: $l^\pm l^\mp q\bar{q}$, $l^\pm \nu^{(-)} q\bar{q}$, and $\nu\bar{\nu} q\bar{q}$. This analysis [8] is based on the $\nu\bar{\nu} q\bar{q}$ final state, and is sensitive to leptoquarks of all three generations. In a previous study of this final state [9] with the assumed decay $LQ \rightarrow \nu q$, DØ set limits of $m_{LQ} > 79 \text{ GeV}/c^2$ for scalar leptoquarks, and $m_{LQ} > 144 \text{ GeV}/c^2$, $159 \text{ GeV}/c^2$, and $206 \text{ GeV}/c^2$, for vector leptoquarks with couplings that correspond to σ_{\min} , MV, and YM couplings, respectively [9,10]. The present analysis is based on a factor of ten increase in data over the previous analysis. The CDF collaboration has conducted a search for second and third generation leptoquarks, also assuming the decay $LQ \rightarrow \nu q$, and set mass limits of 123 (148) GeV/c^2 for second (third) generation scalar leptoquarks, and 171 (199) GeV/c^2 and 222 (250) GeV/c^2 for second (third) generation vector leptoquarks with MV and YM couplings, respectively [11]. The OPAL collaboration has searched $\sqrt{s}=183 \text{ GeV}$ e^+e^- collisions for vector and scalar leptoquarks with specific weak isospins and decay modes [12]. For first and second generation scalar leptoquarks with weak isospin of 1 and the decay $LQ \rightarrow \nu q$, OPAL has set a mass limit of $84.8 \text{ GeV}/c^2$. For other values of weak isospin, the mass limit ranges from $71.6 \text{ GeV}/c^2$ to $80.8 \text{ GeV}/c^2$. Our new results extend the range of sensitivity of the vector leptoquark searches and the first generation scalar leptoquark searches.

The DØ detector [13] consists of three major subsystems: an inner detector for tracking charged particles; an uranium/liquid-argon calorimeter for measuring electromagnetic and hadronic showers; and a muon spectrometer. The inner detector consists of two outer drift chambers separately covering the regions $|\eta| < 1$ and $1.2 < |\eta| < 2.8$, and an inner drift chamber covering the region $|\eta| < 2$. The calorimeter consists of three cryostats supplemented with scintillators between the cryostats. The Main Ring beam pipe used to accelerate and inject protons and antiprotons into the Tevatron traverses the hadronic region of the calorimeter at $\phi=100^\circ$. The jets measured with the calorimeter have a resolution of approximately $\delta E = 0.8\sqrt{E}$ (E in GeV). We measure the missing transverse energy (\cancel{E}_T) by summing the calorimeter energy vectorially in the plane transverse to the beam. The projection of \cancel{E}_T on a given axis has a resolution of $\delta \cancel{E}_{x,y} = 1.08 \text{ GeV} + 0.019(\sum |E_{x,y}|)$ ($E_{x,y}$ in GeV).

The event sample for our search is collected with a trigger requiring a jet with $E_T > 25 \text{ GeV}$, a second jet with $E_T > 10 \text{ GeV}$, $\cancel{E}_T > 25 \text{ GeV}$, and the azimuthal angle between any jet and $\cancel{E}_T(\Delta\phi(\text{jet}, \cancel{E}_T))$ greater than 14.3° . The trigger does not collect data in the 0.4

seconds following Main Ring injection, or within 800 nanoseconds of protons or antiprotons passing through the detector. We remove data affected by accelerator noise or detector malfunctions. The former are identified by significant energy measurement in the region surrounding the Main Ring. The latter are identified by recurring energy measurement in a particular region of the calorimeter, by energy measurement isolated to a single calorimeter cell, and by documented subsystem malfunctions. The integrated luminosity for this sample corresponds to $85.2 \pm 3.7 \text{ pb}^{-1}$.

We select events with well-understood trigger efficiency by requiring at least two jets with $E_T > 50 \text{ GeV}$, $\cancel{E}_T > 40 \text{ GeV}$, $\Delta\phi(\text{jet}, \cancel{E}_T) > 30^\circ$, and $\Delta\mathcal{R}(\text{jet}, \text{jet}) > 1.5$, where $\Delta\mathcal{R} = \sqrt{(\Delta\eta)^2 + (\Delta\phi)^2}$, η is the jet pseudorapidity, and ϕ is the jet azimuthal angle. Jets are defined as the calorimeter energy within a $\Delta\mathcal{R} = 0.5$ cone. We reduce cosmic-ray backgrounds by rejecting events containing jets with little energy in the electromagnetic sections of the calorimetry. Backgrounds arising from W or Z boson production are reduced by rejecting events with isolated muons or jets with a large fraction of their energy measured in the electromagnetic calorimeter.

The remaining backgrounds in the sample consist of events with jets produced in association with a W or a Z boson, and events from top quark and multijet production. We use Monte Carlo generators to simulate the kinematics and topologies of events with W or Z bosons or top quarks, and a GEANT-based simulation [14] of the detector to predict the acceptance for these events.

The W and Z backgrounds correspond to processes involving only neutrinos and jets ($Z + 2 \text{ jets} \rightarrow \nu\nu + 2 \text{ jets}$ and $W + \text{jet} \rightarrow \tau\nu + \text{jet}$, with $\tau \rightarrow \text{hadrons} + \nu$), processes with undetected charged leptons ($W + 2 \text{ jets} \rightarrow l^\pm\nu + 2 \text{ jets}$, $Z + 2 \text{ jets} \rightarrow \mu\mu + 2 \text{ jets}$, and $Z + \text{jet} \rightarrow \tau\tau + \text{jet}$, with one $\tau \rightarrow \text{hadrons} + \nu$), and processes in which an electron is misidentified as a jet ($W + \text{jet} \rightarrow e\nu + \text{jet}$ and $W + \text{jet} \rightarrow \tau\nu + \text{jet}$, with $\tau \rightarrow e\nu\nu$). We use the PYTHIA Monte Carlo generator [15] to generate the $W/Z + \text{jet}$ processes, and the VECBOS Monte Carlo generator [16] to generate the $W/Z + 2 \text{ jets}$ processes. We scale the generator cross sections to match the corresponding $W/Z + \text{jet(s)}$ cross sections measured using decays into electrons. These cross sections were remeasured specifically for this analysis.

To obtain the background from $t\bar{t}$, $t\bar{b}$, and $\bar{t}b$ production, where the top quark decays to an unobserved charged lepton, a neutrino, and a jet, we use our measured cross section for $t\bar{t}$ production [17], and the calculated next-to-leading-order cross section for the single-top production processes [18]. We use the HERWIG Monte Carlo [19] program to generate $t\bar{t}$ events and the CompHEP Monte Carlo [20] program to generate $t\bar{b}$ and $\bar{t}b$ events.

The multijet background arises primarily from a mismeasurement of the interaction vertex or of jet energy. To reduce the number of events with mismeasured vertices, we use the central drift chamber (CDC) to associate tracks with the two highest E_T jets, if those jets are in the fiducial volume of the CDC ($|\eta| \leq 1$). These tracks are used to determine the point-of-origin of each jet, which is required to be no further than 15 cm from the reconstructed event vertex (the latter is determined from all tracks in the event). The 15 cm value is chosen to maximize the inverse of the fractional uncertainty on signal (see below). We reduce the number of events with poorly measured jet energies by requiring that the azimuth $\Delta\phi$ between the \cancel{E}_T vector and the direction of the jet with the second highest E_T exceed 60° . Table I shows the number of events remaining in the data after each additional selection criterion.

Selection criterion	# of Events
2 Jets + \cancel{E}_T Trigger	503,557
No accelerator noise or detector malfunctions	399,557
Leading jet $E_T \geq 50$ GeV	236,339
Second jet $E_T \geq 50$ GeV	86,826
$\cancel{E}_T \geq 40$ GeV	8,996
$\Delta\phi(\text{jet}, \cancel{E}_T) \geq 30^\circ$	1,567
$\Delta\mathcal{R}(\text{jet}, \text{jet}) > 1.5$	1,495
Jet EM Fraction cuts	1,358
No isolated muons	1,332
Leading or second jet $ \eta \leq 1.0$; all jets $ \eta \leq 4.0$	1,071
Jet vertex - Primary vertex < 15 cm	401
$\Delta\phi(\text{jet 2}, \cancel{E}_T) \geq 60^\circ$	231

TABLE I. The set of criteria imposed on the 2 jets + \cancel{E}_T data sample and the number of events that pass each additional selection criterion.

To estimate the remaining multijet background in our search sample, we count events in which jet-based vertex positions deviate by 15 cm to 50 cm from the position of the event vertex. In events with two central ($|\eta| \leq 1$) jets, we require both vertices to fall within this range. We normalize these events to the search sample using a multijet-dominated sample ($\Delta\phi(\text{jet 2}, \cancel{E}_T) < 60^\circ$). The expected multijet background is:

$$N_{mj} = N_{\Delta\phi > 60^\circ}^{15 < z < 50} \left(\frac{N^{z < 15}}{N^{15 < z < 50}} \right)_{\Delta\phi < 60^\circ}$$

We choose the upper bound of 50 cm to provide the best match between expected background and data for events with \cancel{E}_T between 30 GeV and 40 GeV, a region dominated by multijet events. We predict 162.8 ± 23.7 multijet and 51.9 ± 7.0 W , Z , and top events in this sample. We observe 224 events in the data. Changing the vertex threshold to 100 cm increases the multijet background prediction by 22% in this region, which we take as an estimate of the systematic error of the method. Table II shows the total expected background and the observed number of events for the final 2 jets + \cancel{E}_T data sample.

To model the characteristics of leptoquark production, we use scalar leptoquark events generated with the PYTHIA Monte Carlo program and vector leptoquark events generated with the CompHEP Monte Carlo program. The cross sections for scalar leptoquark production have been calculated to next-to-leading order [21], while those for vector leptoquark production have been calculated to leading order [22]. The calculations use a QCD renormalization and factorization scale of $\mu = m_{LQ}$, with theoretical uncertainties estimated by changing the scale to $\mu = m_{LQ}/2$ and $\mu = 2m_{LQ}$. For scalar leptoquarks we use the smaller predicted cross section ($\mu = 2m_{LQ}$) for determining the mass limits on LQ 's.

Failure to observe any hypothetical signal at 95% confidence level (C.L.) corresponds approximately to a downward fluctuation of that signal by two standard deviations. Hence,

to increase the sensitivity of our search for the production of leptoquarks that decay to νq , we search for leptoquarks that would produce excesses of approximately two standard deviations. We separately optimize our selection criteria for the production of 100 GeV/c^2 scalar leptoquarks and for 200 GeV/c^2 vector leptoquarks with Minimal Vector coupling. Other choices of leptoquark masses do not significantly affect our results. We use the JETNET [23] neural network program to isolate regions of significant leptoquark production, with \cancel{E}_T and $\Delta\phi(\text{jet}, \text{jet})$ as inputs for scalar leptoquarks, and \cancel{E}_T and the E_T of the jet with the second highest E_T as inputs for vector leptoquarks. The values of the neural network output variables and the thresholds for these masses are shown in Fig. 1. The thresholds are chosen to maximize the quantity:

$$\frac{N_{lq}}{\sqrt{N_{lq} + N_{\text{back}} + (\Delta N_{lq})^2 + (\Delta N_{\text{back}})^2}},$$

where N_{lq} and N_{back} are the number of signal and background events, respectively, and ΔN_{lq} and ΔN_{back} are their associated uncertainties. This quantity reflects the inverse of the fractional uncertainty on signal. After applying these thresholds, we expect $56.0^{+8.1}_{-8.2}$ events and observe 58 events for the scalar leptoquark optimization, and expect $13.3^{+2.8}_{-2.6}$ events and observe 10 events for the vector leptoquark optimization.

Type of Events	# of Events
Multijet	$58.8 \pm 14.1 \pm 12.9$
$(W \rightarrow e\nu) + \text{jet}$	$51.9 \pm 7.0 \pm^{13.7}_{-8.9}$
$(W \rightarrow \tau\nu) + \text{jet}$	$46.3 \pm 5.0 \pm^{8.9}_{-7.7}$
$(Z \rightarrow \nu\nu) + 2 \text{ jets}$	$36.1 \pm 7.7 \pm^{9.0}_{-5.5}$
$(W \rightarrow \mu\nu) + 2 \text{ jets}$	$18.7 \pm 3.5 \pm^{4.2}_{-3.7}$
$t\bar{t} \rightarrow l^\pm\nu + 4 \text{ jets}$	$10.6 \pm 2.0 \pm 2.3$
$(W \rightarrow e\nu) + 2 \text{ jets}$	$8.3 \pm 2.5 \pm^{2.0}_{-2.5}$
$(W \rightarrow \tau\nu) + 2 \text{ jets}$	$5.6 \pm 1.7 \pm^{1.4}_{-0.8}$
$tb \rightarrow l^\pm\nu + 2 \text{ jets}$	$2.0 \pm 0.3 \pm 0.2$
$(Z \rightarrow \tau\tau) + \text{jet}$	$2.0 \pm 0.4 \pm^{0.6}_{-0.3}$
$(Z \rightarrow \mu\mu) + 2 \text{ jets}$	$1.7 \pm 0.4 \pm^{0.4}_{-0.3}$
Total background	$242.0 \pm 18.9 \pm^{23.3}_{-19.3}$
Data	231

TABLE II. The expected and observed numbers of events in the final 2 jets + \cancel{E}_T sample.

After applying the optimal thresholds, we find that the observed number of events is consistent with the expected background, and that, consequently, we have no evidence for leptoquark production. This null result yields the 95% C.L. upper limit on cross section (Fig. 2) as a function of leptoquark mass. We calculate the limit using a Bayesian method [24] with a flat prior for the signal and Gaussian priors for background and acceptance

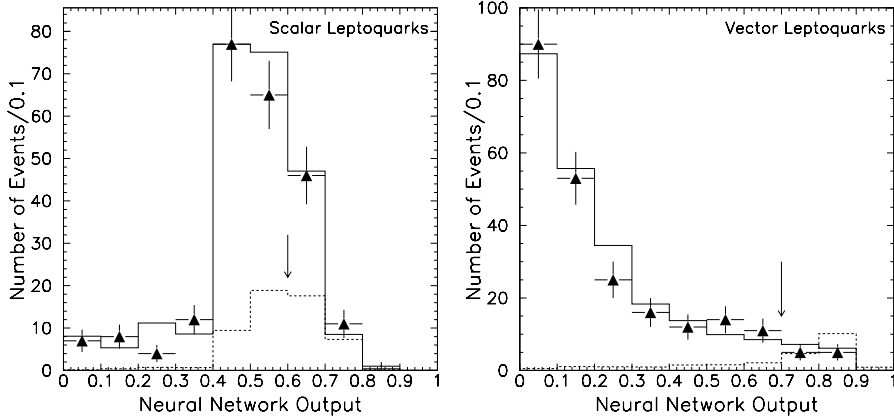


FIG. 1. The neural network output for data (points), for background (solid histogram), and for leptoquarks (dashed histogram). The optimization is for $100 \text{ GeV}/c^2$ scalar leptoquarks (left) and $200 \text{ GeV}/c^2$ vector leptoquarks with Minimal Vector coupling (right). We remove events to the left of the arrows.

uncertainties. The equivalent limits on mass are $98 \text{ GeV}/c^2$ for scalar leptoquarks, and $200 \text{ GeV}/c^2$, $238 \text{ GeV}/c^2$, and $298 \text{ GeV}/c^2$ for vector leptoquarks with couplings corresponding to the minimum cross section σ_{\min} , Minimal Vector coupling, and Yang-Mills coupling, respectively. We summarize the DØ mass limits as a function of the branching fraction $\mathcal{B}(LQ \rightarrow l^\pm q)$ for first [9] and second [25] generation leptoquarks in Fig. 3. These limits combine searches using the final states $l^\pm l^\mp q\bar{q}$, $l^\pm \nu^{(-)} q\bar{q}$, and $\nu\bar{\nu}q\bar{q}$. We note that the gap at small values of $\mathcal{B}(LQ \rightarrow l^\pm q)$ in previous analyses has been filled as a result of this investigation.

We thank the staffs at Fermilab and collaborating institutions, and acknowledge support from the Department of Energy and National Science Foundation (USA), Commissariat à L'Energie Atomique and CNRS/Institut National de Physique Nucléaire et de Physique des Particules (France), Ministry for Science and Technology and Ministry for Atomic Energy (Russia), CAPES and CNPq (Brazil), Departments of Atomic Energy and Science and Education (India), Colciencias (Colombia), CONACyT (Mexico), Ministry of Education and KOSEF (Korea), CONICET and UBACyT (Argentina), The Foundation for Fundamental Research on Matter (The Netherlands), PPARC (United Kingdom), Ministry of Education (Czech Republic), and the A.P. Sloan Foundation.

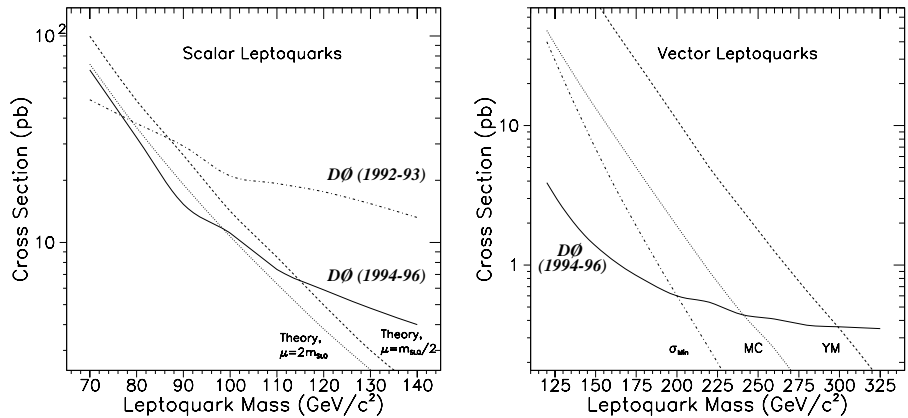


FIG. 2. Limits on cross section at 95% confidence level, as a function of leptoquark mass, for scalar (top) and vector (bottom) leptoquarks, and different theoretical predictions. We assume the LQ decays exclusively to νq . The theoretical predictions correspond to the production of leptoquarks of a single generation, while the experimental limit corresponds to the sum of contributions from leptoquarks of all three generations.

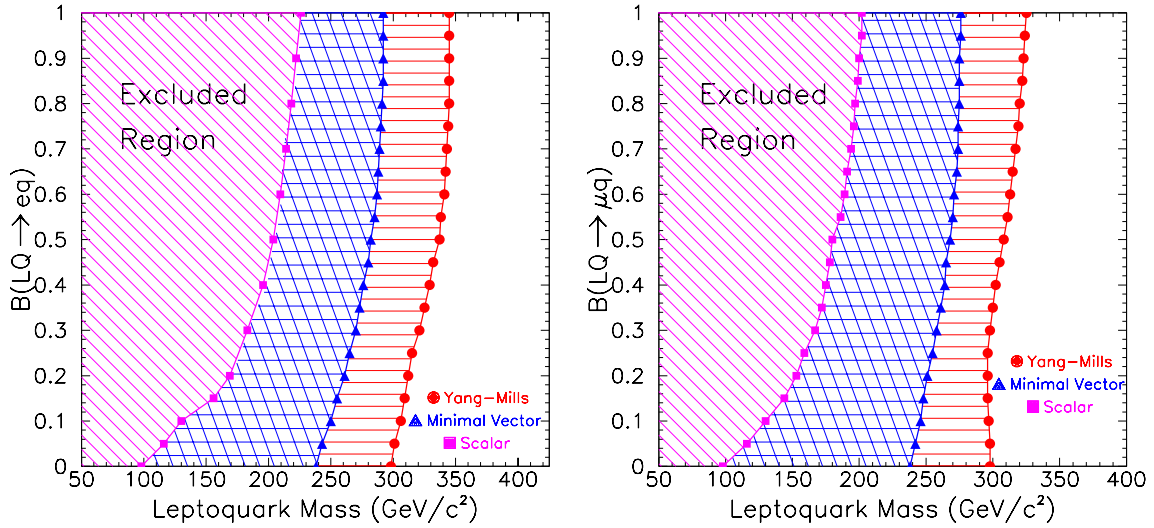


FIG. 3. The region of $B(LQ \rightarrow l^\pm q)$ vs. mass for first-generation (top) and second-generation (bottom) leptoquarks excluded by DØ.

REFERENCES

* Visitor from University of Zurich, Zurich, Switzerland.
† Visitor from Institute of Nuclear Physics, Krakow, Poland.

- [1] H. Georgi and S. Glashow, Phys. Rev. Lett. **32**, 438 (1974); J.C. Pati and A. Salam, Phys. Rev. D **10**, 275 (1974).

- [2] P.H. Frampton, Mod. Phys. Lett. A **7**, 559 (1992).
- [3] J. L. Hewett and T. G. Rizzo, Phys. Rep. **183**, 193 (1989); E. Accomando *et al.*, Phys. Rep. **299**, 1 (1998).
- [4] E. Eichten and K. Lane, hep-ph/9609297; hep-ph/9609298, Proceedings of 1996 Snowmass Summer Study.
- [5] D. Choudhury and S. Raychaudhuri, Phys. Lett. B **401**, 367 (1997); G. Altarelli *et al.*, Nucl. Phys. B **506**, 3 (1997).
- [6] J. Blümlein, E. Boos, and A. Kryukov, Z. Phys. C **76**, 137 (1997).
- [7] H.-U. Bengtsson, W.-S. Hou, A. Soni, and D. H. Stork, Phys. Rev. Lett. **55**, 2762 (1985).
- [8] C. Hays, Ph.D. thesis, Columbia University, 2001 (unpublished).
- [9] B. Abbott *et al.*(DØ Collaboration), Phys. Rev. Lett. **80**, 2051 (1998).
- [10] V. M. Abazov *et al.*(DØ Collaboration), hep-ex/0105072.
- [11] T. Affolder *et al.*, Phys. Rev. Lett. **85**, 2056 (2000).
- [12] G. Abbiendi *et al.*, Eur. Phys. J. C **13**, 15 (2000).
- [13] B. Abbott *et al.* (DØ Collaboration), Nucl. Instrum. Methods Phys. Res. A **338**, 185 (1994).
- [14] R. Brun and F. Carminati, CERN Program Library Long Writeup, W5013, 1993 (unpublished). We used version 3.15.
- [15] T. Sjöstrand, Comput. Phys. Commun. **82**, 74 (1994). We used version 6.127.
- [16] F.A. Berends *et al.*, Nucl. Phys. B**357**, 32 (1991).
- [17] B. Abbott *et al.* (DØ Collaboration), Phys. Rev. D **60**, 012001 (1999).
- [18] M.C. Smith and S. Willenbrock, Phys. Rev. D **54**, 6696 (1996); T. Stelzer, Z. Sullivan, and S. Willenbrock, Phys. Rev. D **56**, 5919 (1997); *ibid.* **58**, 094021 (1998); V. M. Abazov *et al.*, Phys. Lett. B **517**, 282 (2001).
- [19] G. Marchesini *et al.*, Comput. Phys. Commun. **67**, 465 (1992).
- [20] A. Pukhov *et al.*, hep-ph/9908288. We used version 3.0.
- [21] M. Krämer *et al.*, Phys. Rev. Lett. **79**, 341 (1997).
- [22] J. Blümlein, E. Boos, and A. Kryukov, hep-ph/9811271.
- [23] C. Peterson, T. Rögnvaldsson, and L. Lönnblad, Comput. Phys. Commun. **81**, 185 (1994). We used version 3.4.
- [24] I. Bertram *et al.*, Fermilab-TM-2104 (unpublished).
- [25] B. Abbott *et al.* (DØ Collaboration), Phys. Rev. Lett. **84**, 2088 (2000).